Langmuir Article

pubs.acs.org/Langmuir

Aliphatic Hyperbranched Polyester: A New Building Block in the Construction of Multifunctional Nanoparticles and Nanocomposites

Santimukul Santra,[†] Charalambos Kaittanis,[†,‡] and J. Manuel Perez*[,†,‡,§]

[†]*Nanoscience Technology Center,* [‡]*Burnett School of Biomedical Sciences, College of Medicine, and* [§]*Department of Chemistry, University of Central Florida, 12424 Research Parkway, Suite 400, Orlando, Florida 32826*

Received October 6, 2009. Revised Manuscript Received November 11, 2009

Herein we report the design and synthesis of multifunctional hyperbranched polyester-based nanoparticles and nanocomposites with properties ranging from magnetic, fluorescence, antioxidant and X-ray contrast. The fabrication of these nanostructures was achieved using a novel aliphatic and biodegradable hyperbranched polyester (HBPE) synthesized from readily available diethyl malonate. The polymer's globular structure with functional surface carboxylic groups and hydrophobic cavities residing in the polymer's interior allows for the formation of multifunctional polymeric nanoparticles, which are able to encapsulate a diversity of hydrophobic cargos. Via simple surface chemistry modifications, the surface carboxylic acid groups were modified to yield nanoparticles with a variety of surface functionalizations, such as amino, azide and propargyl groups, which mediated the conjugation of small molecules. This capability achieved the engineering of the HBPE nanoparticle surface for specific cell internalization studies and the formation of nanoparticle assemblies for the creation of novel nanocomposites that retained, and in some cases enhanced, the properties of the parental nanoparticle building blocks. Considering these results, the HBPE polymer, nanoparticles and composites should be ideal for biomedical, pharmaceutical, nanophotonics applications.

Introduction

The design of multifunctional polymeric nanoparticles is an emerging field with important applications in catalysis, sensing, optics, material design, drug delivery and imaging.[1−4] Nanoparticles that combine multiple materials or encapsulate a variety of guest molecules can be used to incorporate unique properties to these nanostructures.[5] Furthermore, assemblies of multifunctional nanoparticles can be engineered to obtain supramolecular assemblies with combined or enhanced properties, derived from both the type and amount of the constituent polymeric nanoparticles used in the assembly.[6−8] A variety of polymeric matrices has been used to synthesize polymeric nanoparticles, but oftentimes the diversity of the encapsulated molecules is compromised by the nature of the polymeric matrix itself that limits the amount and kind of guest molecule to be encapsulated. In addition, the surface functionalization of the resulting nanoparticle is limited by the use of complex and non-reproducible conjugation chemistries.

Hyperbranched polymers (HBPs) composed of densely branched structures adopt compact conformations with a large number of surface reactive groups.[9−13] Their easy one-step synthesis, oftentimes involving the condensation of AB_2 type monomers, contrasts with the more complex synthesis of other types of highly branched macromolecules, such as dendrimers. One important feature of these HBPs, particularly those made with a polyester backbone, is their high solubility in common polar solvents (e.g., DMF, DMSO, acetone), which makes them ideal for the development of hyperbranched polyester (HBPE) nanostructures, such as polymeric nanoparticles, by the solvent diffusion method.[14,15] These HBPE nanoparticles would have the benefits of being globular in nature, highly functionalized, biodegradable and able to encapsulate a variety of guest molecules in their nanocavities located within the inner branches of the polymeric coating.

Acknowledging the benefits of HBPE and HBPE nanoparticles, herein we report the design and synthesis of an aliphatic hyperbranched polyester with hydrophobic cavities and hydrophilic surface and its application in the development of multifunctional nanoparticles and nanocomposites (Scheme 1). To the best of our knowledge, this is the first time that this type of structure (**4**) has been utilized to synthesize a novel HBPE polymer suitable for the fabrication of theranostic polymeric nanoparticles with high surface functional groups. This functional AB_2 monomer is designed in such a way that under polymerization conditions it grows three dimensionally, forming a highly branched polymeric structure. In addition, this is the first example of an aliphatic and spherical-shaped hyperbranched polyester that utilizes the solvent diffusion method[14,15] for the synthesis of multifunctional

*Corresponding author. Telephone: 407-882-2843. Fax: 407-882-2819. E-mail: jmperez@mail.ucf.edu.

(1) Nayak, S.; Lee, H.; Chmielewski, J.; Lyon, L. A. *J. Am. Chem. Soc.* **2004**, *126*, 10258–10259.
(2) Kim, C. K.; Ghosh, P.; Pagliuca, C.; Zhu, Z. J.; Menichetti, S.; Rotello, V. M. *J. Am. Chem. Soc.* **2009**, *131*, 1360–1361.
(3) You, C. C.; Miranda, O. R.; Gider, B.; Ghosh, P. S.; Kim, I. B.; Erdogan, B.; Krovi, S. A.; Bunz, U. H.; Rotello, V. M. *Nat. Nanotechnol.* **2007**, *2*, 318–323.
(4) Marder, S. R.; Kippelen, B.; Jen, A. K. Y.; Peyghambarian, N. *Nature* **1997**, *388*, 845–851.
(5) Peer, D.; Karp, J. M.; Hong, S.; Farokhzad, O. C.; Margalit, R.; Langer, R. *Nat. Nanotechnol.* **2007**, *2*, 751–760.
(6) Iyer, A. S.; Lyon, L. A. *Angew. Chem., Int. Ed. Engl.* **2009**, *48*, 4562–4566.
(7) Nayak, S.; Lyon, L. A. *Angew. Chem., Int. Ed. Engl.* **2005**, *44*, 7686–7708.
(8) Boal, A. K.; Ilhan, F.; DeRouchey, J. E.; Thurn-Albrecht, T.; Russell, T. P.; Rotello, V. M. *Nature* **2000**, *404*, 746–748.
(9) Duncan, R. *Nat. Rev. Drug. Discov.* **2003**, *2*, 347–360.
(10) Lee, C. C.; MacKay, J. A.; Frechet, J. M.; Szoka, F. C. *Nat. Biotechnol.* **2005**, *23*, 1517–1526.
(11) Santra, S.; Kumar, A. *Chem. Commun.* **2004**, 2126–2127.
(12) Marco Fischer, F. V. *Angew. Chem., Int. Ed.* **1999**, *38*, 884–905.
(13) Frechet, J. M. J.; Henmi, M.; Gitsov, I.; Aoshima, S.; Leduc, M. R.; Grubbs, R. B. *Science* **1995**, *269*, 1080–1083.
(14) McCarthy, J. R.; Perez, J. M.; Bruckner, C.; Weissleder, R. *Nano. Lett.* **2005**, *5*, 2552–2556.
(15) Packard, B. S.; Wolf, D. E. *Biochemistry* **1985**, *24*, 5176–5181.

Scheme 1. Schematic Representation of the Three Dimensional Structure of the Aliphatic Hyperbranched Polymer (HBPE 5) and Its HBPE Nanoparticles[a]

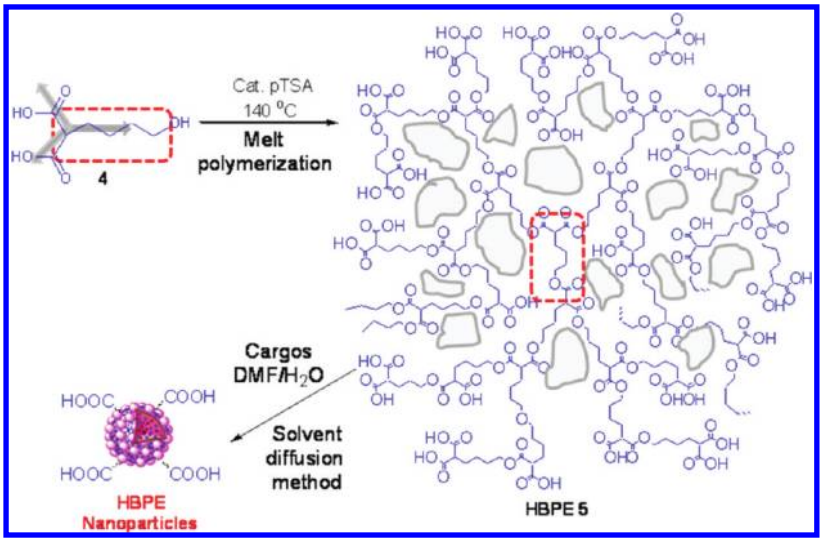

[a] Monomer **4** has three-bond connectivity (the arrows) to grow three-dimensionally under polymerization conditions, resulting in a highly branched polymer with hydrophobic cavities in the polymeric structure.

polymeric nanoparticles. Furthermore, our HBPE can be easily synthesized in one-pot as opposed to dendrimers (e.g., PAMAM dendrimers) that involve iterative synthetic steps. Our synthesized new HBPE polyester can be easily modified to ultimately yield a library of functional nanoparticles for the development of multifunctional nanocomposites.

The as-synthesized spherical-shaped, highly branched polymer has internal hydrophobic cavities (polymer cavities) that provide high affinity for the encapsulation of various hydrophobic guest molecules and the polymer surface consists of polar carboxylic acid groups that can be further functionalized to generate a library of functional hyperbranched polymer using "click" chemistry and carbodiimide chemistry. Because of their surface functionalities, the nanoparticles can be conjugated with functional ligands to (i) target and (ii) self-assemble with other nanoparticles to create multifunctional nanocomposites.

Experimental Section

Materials. Dry DMF, DMSO, 3-(4,5-dimethylthiazol-2-yl)-2,5-diphenyltetrazolium bromide (MTT), 1,1′-carbonyldiimidazole (CDI), *N*-hydroxysuccinimide (NHS), AZT (azidothymidine), diethyl malonate, and other chemicals were purchased from Sigma-Aldrich and used without further purification. Near infrared dyes (DiI-D282, DiD-D7757, and DiR-D12731) and 4′,6-diamidino-2-phenylindole (DAPI-D1306) were purchased from Invitrogen, whereas the EDC (1-ethyl-3-[3-(dimethylamino)propyl] carbodiimide hydrochloride) was obtained from Pierce Biotechnology. The human lung carcinoma cell line A549 (CCL-185) and cardiomyocytes (H9c2) were obtained from ATCC. Dialysis membranes were obtained from Spectrum Laboratories. Acetonitrile, tetrahydrofuran, and other solvents were purchased from Fisher Scientific and used as received, unless otherwise stated.

Characterizations. Infrared spectra were recorded on a PerkinElmer Spectrum 100 FT-IR spectrometer. UV/vis spectra were recorded using a CARY 300 Bio UV/vis spectrophotometer. Fluorescence spectra were recorded on a NanoLog Horiba Jobin Yvon fluorescence spectrophotometer. NMR spectra were recorded on a MERCURY 300 MHz spectrometer using the TMS/solvent signal as an internal reference. Gel permeation chromatography (GPC) results were obtained using a JASCO MD 2010 Plus instrument with a PD 2020 light scattering Precision Detector. Thermo gravimetric analyses (TGA) were performed on a SETARAM, Mettler TC11 instrument with sample sizes of 10−20 mg. All experiments were done using a heating rate of 10 °C/min in air. The overall surface charge (ζ potential) of the HBPE nanoparticles was measured using a Zetasizer Nano ZS from Malvern Instruments. Confocal images were taken on a Zeiss Axioskop 2 mot plus confocal microscope. Flow Cytometry experiments were performed using a BD FACS Calibur multipurpose flow cytometer system from BD Biosciences. MTT study has been done using the Biotek Synergy HT multi-detection microplate reader. Dynamic light scattering (DLS) studies were done using a PDDLS/CoolBatch 40T instrument and a Precision Deconvolve 32 software. IVIS experiments were done on an IVIS 50 imaging system from Xenogen imaging technologies. Analytical Thin Layer Chromatography (TLC) was performed on glass plates coated with silica gel GF 254 and were visualized in iodine vapor. Column chromatography was performed using silica gel (100−200 mesh), and the eluant is mentioned in the procedures below for each case.

Synthesis. *Synthesis of 4-Bromobutyl Acetate* (**2**). Tetrahydrofuran (12.2 mL, 148.4 mmol) and potassium bromide (21.1 g, 176.5 mmol) were added into a 250 mL round-bottom flask containing 150 mL of acetonitrile. The reaction mixture was cooled to 0 °C, followed by dropwise addition of acetyl chloride (11 mL, 155.1 mmol). Subsequently, the mixture was brought to room temperature, where it was continuously stirred for 36 h. The reaction mixture was poured in water and extracted with ethyl acetate. The organic layer was washed with water, dried over Na_2SO_4, and concentrated in order to obtain the pure product as a colorless liquid.

Yield: 24.3 g (85%). Bp: >250 °C. ^{1}H NMR (300 MHz, $CDCl_3$, δ ppm, J Hz): 1.79 (m, 2H), 1.92 (m, 2H), 2.03 (s, 3H), 3.46 (t, 2H, J = 7.6), 4.08 (t, 2H, J = 6.7). ^{13}C NMR (75 MHz, $CDCl_3$, δ ppm): 20.87, 27.36, 29.36, 33.03, 63.43, 170.95. IR ($CHCl_3$): 3038, 2926, 1352, 1243, 1052 cm^{-1}.

Synthesis of 2-(4-Acetoxybutyl)malonic Acid Diethyl Ester (**3**). Diethyl malonate (**1**) (10 g, 62.5 mmol) and 4-bromobutyl acetate (**2**) (15.84 g, 81.3 mmol) were placed in a round-bottom flask containing acetonitrile (120 mL) and stirred for 2 min at room temperature. Then, potassium carbonate (34.5 g, 250.1 mmol) was added and refluxed for 36 h. Next, the mixture was filtered and the filtrate was concentrated to obtain a yellow liquid. This was extracted with ethyl acetate, and washed with water. The organic layers were combined and dried over Na_2SO_4,

and purified by column chromatography using 4% ethyl acetate in petroleum ether as the eluent.

Yield: 13.02 g (76%). Bp: 250 °C. ^{1}H NMR (300 MHz, $CDCl_3$, δ ppm, J Hz): 1.28 (t, 6H, J = 7.6), 1.38 (m, 2H), 1.62 (q, 2H, J = 7.2), 1.98 (q, 2H, J = 7.7), 2.05 (s, 3H), 3.34 (t, 1H, J = 7.7), 4.09 (t, 2H, J = 6.6), 4.22 (q, 4H, J = 7.2). ^{13}C NMR (75 MHz, $CDCl_3$, δ ppm): 14.06, 20.79, 23.74, 28.25, 28.25, 51.84, 61.27, 63.89, 169.31, 171.11. IR ($CHCl_3$): 2982, 1728, 1463, 1367, 1233, 1151, 1029, 860 cm^{-1}.

Synthesis of 2-(4-Hydroxybutyl)malonic Acid (***4***). 2-(4-Acetoxybutyl)malonic acid diethyl ester (**3**) (5.0 g, 18.25 mmol, see Section S1 in the Supporting Information for the synthesis of compound **3**) was taken in a 100 mL round-bottom flask containing methanol (50 mL) and stirred at room temperature for 2 min. To this solution, NaOH (2.1 g, 54.74 mmol) in water (7 mL) was added and stirred at 90 °C for 8 h. The reaction mixture was brought to room temperature and acidified (pH 2−3) with the dropwise addition of dilute hydrochloric acid at room temperature with constant stirring. The mixture was then concentrated using rotary evaporator and applying vacuum. To the concentrated reaction mixture chloroform (50 mL) was added and Argon gas was bubbled through the solution at 60 °C to remove excess HCl. The mixture was filtered and the filtrate was concentrated. This was then purified by column chromatography using 35% ethyl acetate in petroleum ether as eluent.

Yield: 2.31 g (72%). ^{1}H NMR (300 MHz, $CDCl_3$, δ ppm, J Hz): 1.41 (m, 2H), 1.59 (m, 2H), 1.91 (q, 2H, J_1 = 7.3, J_2 = 7.8), 3.37 (t, 1H, J = 7.4), 3.64 (t, 2H, J = 6.5), 5.54 (bs, 1H). ^{13}C NMR (75 MHz, $CDCl_3$, δ ppm): 23.53, 28.52, 31.75, 52.64, 62.11, 170.55. IR ($CHCl_3$): 3507, 2941, 1710, 1626, 1459, 1438, 1391, 1198, 1157, 1050, 947, 772, 741, 664 cm^{-1}.

Synthesis of Hyperbranched Polyester (*HBPE*) ***5***. The monomer **4** and the catalyst *p*-toluenesulfonic acid (100:1 molar ratio) were taken into a 10 mL round-bottom flask and dried under high vacuum followed by the release of vacuum using dry argon gas. Then the flask was slowly heated to 150 °C under argon atmosphere using an oil bath, and it was kept at this temperature for 2 h. The evolution of the byproduct (water vapor) was clearly visible after the sample was heated at 150 °C. The melted reaction mixture was evacuated at 0.2 mm/Hg for 1 h, while maintaining the same polymerization temperature. The polymer was purified by dissolving in DMF and reprecipitating in methanol. This was then centrifuged, washed with methanol and dried in a high vacuum pump to get pure polymer.

Yield: 65%. ^{1}H NMR (300 MHz, DMSO-d_6, δ ppm): 1.25 (m, 2H), 1.52 (m, 2H), 1.67 (m, 2H), 3.38 (m, 1H), 3.58 (m, 2H), 5.28 (m, 1H). ^{13}C NMR (75 MHz, DMSO-d_6, δ ppm): 23.82, 28.23, 51.85, 52.63, 65.37, 170.45. IR: 2954, 1727, 1458, 1436, 1343, 1218, 1152, 1054, 943, 858, 743, 694 cm^{-1}. TGA: 10% weight loss at 250 °C.

Gel Permeation Chromatography (*GPC*). The molecular weight of the resulting polymer was determined using Gel Permeation Chromatography (GPC). The average molecular weight was calculated against a polystyrene standard, using HPLC-grade DMF as the mobile phase. For a comparative study between the average molecular weight (M_w) and the polymerization time at 150 °C, the samples were taken from the reaction mixture periodically and analyzed by GPC. With increase in time there was an increase in the molecular weight, whereas a dramatic increase in the polymer's molecular weight was observed when high vacuum was applied. The average molecular weight of the polymer **5** was M_w = 42 000, PD = 1.6, whereas only oligomers and low molecular weight polymers were obtained before applying vacuum.

Post-functionalizations of HBPE 5: Carbodiimide Chemistry. The water insoluble carbodiimide 1,1′-carbonyldiimidazole (CDI) was used for the synthesis of aminated (**6**), alkynated (**7**), and azide-functionalized (**8**) hyperbranched polymers. The resulting polymers were found to be soluble in DMF and DMSO.

Synthesis of Hyperbranched Polyester Amine (*HBPE−EDA*) ***6***. The polymer **5** (0.1 g, 0.0025 mmol) was dissolved in dry DMF (1 mL) and CDI (0.041 g, 0.25 mmol) in dry DMF (0.1 mL) was added dropwise. The reaction mixture was incubated for 2 h at room temperature. Ethylenediamine (0.015 g, 0.25 mmol) in dry DMF (0.4 mL) was then added dropwise to the reaction mixture and incubated at room temperature for 24 h. The resulting reaction mixture was then precipitated in methanol, centrifuged and dried in a vacuum pump to get the pure aminated polymer.

Yield: 88%. ^{1}H NMR (300 MHz, DMSO-d_6, δ ppm): 1.27 (m, 2H), 1.55 (m, 2H), 1.74 (m, 2H), 2.26 (m, 4H), 2.88 (m, 4H), 3.34 (m, 1H), 3.63 (m, 4H), 4.04 (m, 2H). IR: 3245, 2940, 2864, 1725, 1659, 1534, 1435, 1240, 1159, 1062, 1021, 952, 929, 826, 749, 704, 663 cm^{-1}.

Synthesis of Alkynated Hyperbranched Polyester (*HBPE−PA*) ***7***. A similar procedure has been followed as described for the synthesis of polymer **6**. Instead of ethylenediamine, propargylamine (0.014 g, 0.25 mmol) was used as the starting material.

Yield: 80%. ^{1}H NMR (500 MHz, DMSO-d_6, δ ppm): 1.28 (m, 2H), 1.54 (m, 2H), 1.75 (m, 2H), 2.25 (m, 2H), 3.42 (bs, 1H), 3.96 (m, 4H), 4.03 (m, 2H). IR: 3121, 2954, 2698, 2215, 1728, 1705, 1664, 1530, 1458, 1437, 1326, 1260, 1165, 1094, 1065, 827, 748 cm^{-1}.

Synthesis of Azide-Functionalized Hyperbranched Polyester (*HBPE−APA*) ***8***. Similar procedure has been followed as described for the synthesis of polymer **6**. Instead of ethylenediamine, aminopropyl azide (0.025 g, 0.25 mmol) was used as the starting material. Aminopropyl azide was prepared using the previously reported method.[27]

Yield: 84%. ^{1}H NMR (500 MHz, DMSO-d_6, δ ppm): 1.29 (m, 6H), 1.49 (m, 6H), 1.80 (m, 2H), 3.21 (m, 4H), 3.39 (bs, 1H), 4.01 (m, 2H). IR (Neat): 3217, 2949, 2098, 1730, 1669, 1599, 1391, 1260, 1165, 1066, 834, 757, 665 cm^{-1}.

Synthesis and Characterizations of Cargo Encapsulated HBPE Nanoparticles: Water-Based Solvent Diffusion Method. *Synthesis of Cargo-Encapsulating Polymeric Nanoparticles* (***9−12***). Here, 5 μL solutions of different near IR dyes (DiI, DiR or DiD, 10 μg/μL), chelated metals (DOTA−Gd, 25 μg/μL), and iodinated molecules (5-amino-2,4,6-triiodoisophthalic acid, 50 μg/μL) in 250 μL of DMF were separately mixed into 250 μL of DMF solution containing hyperbranched polymers (**5**, **6**, **7**, and **8**, 0.025 g) and vortexed. The resulting polymer-cargos mixture in DMF was added dropwise to deionized water (5 mL) with continuous stirring at room temperature forming cargos encapsulating HBPE nanoparticles. The synthesized nanoparticles (**9**−**12**) were purified using a PD-10 column and finally dialyzed (MWCO 6−8K) against PBS (pH = 7.4).

Synthesis of Taxol and DiI Coencapsulating Polymeric Nanoparticles (***9***, ***11***). Taxol (5 μL, 1 μg/μL) and DiI dye (5 μL, 10 μg/μL) were taken in a tube containing either carboxylated (**5**) or alkynated (**7**) polymer (0.025 g) in 500 μL of DMF, and the solvent diffusion method was followed as described above.

Synthesis of AzT and DiI Coencapsulating Polymeric Nanoparticles (***9***, ***11***). AzT (azidothymidine, 5 μL, 1 μg/μL) and DiI dye (5 μL, 10 μg/μL) were taken in an Eppendorf tube containing either carboxylated (**5**) or alkynated (**7**) polymer (0.025 g) in 500 μL of DMF, and the solvent diffusion method was followed as described above.

*Synthesis of Functional HBPE Nanoparticles **10**, **11**, and **12**: Water-Soluble EDC Chemistry*. Alternatively, different surface functional HBPE nanoparticles (**10**, **11** and **12**) can be prepared from carboxylated HBPE nanoparticles (**9**, Supporting Information Scheme S1) using water-soluble EDC [1-ethyl-3-(3-(dimethylamino)propyl) carbodiimide hydrochloride]

Scheme 2. Schematic Representation of the Syntheses of Functional Hyperbranched Polyesters (5−8) and HBPE Nanoparticles (HBPE-NPs 9−12) Using the Melt Polymerization Technique and the Solvent Diffusion Method, Respectively[a]

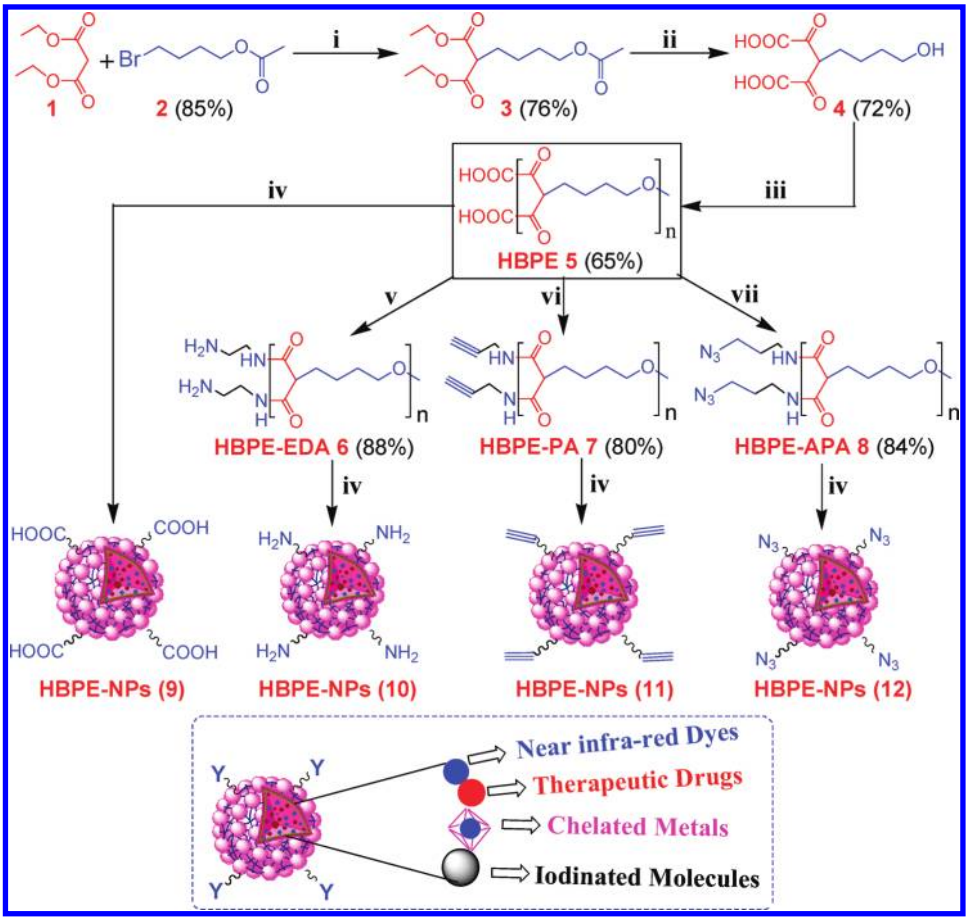

[a] "Click" and carbodiimide chemistry has been used for the syntheses of the library of functional HBPE nanoparticles.

chemistry, following previously reported method.[27] Briefly, to a solution of carboxylated HBPE nanoparticles (**9**, 1.0 mol) in MES buffer, a solution of EDC (10 mmol) and NHS (10 mmol) was added followed by 3 min incubation at room temperature. Ethylenediamine, propargylamine or aminopropyl azide (10 mmol) in DMF were then added dropwise and continued for 3 h to obtain **10**, **11**, or **12**, respectively.

*Synthesis of Folate-Functionalized Polymeric Nanoparticle **13**: "Click" Chemistry*. The alkynated HBPE nanoparticles **11** (0.025 g, 6×10^{-3} mmol) in bicarbonate buffer (pH = 8.5) were taken to an Eppendorf containing catalytic amount of CuI (0.11 μg, 6×10^{-10} mmol) in 250 μL of bicarbonate buffer (pH = 8.5), vortexed for 30 s (Supporting Information Scheme S2). To this, azide-functionalized folic acid (0.003 g, 6×10^{-2} mmol) in DMSO was added and the reaction was incubated at room temperature for 12 h. The synthesized HBPE nanoparticles (**13**) were purified using a PD-10 column and finally dialyzed (MWCO 6−8K) against PBS solution (pH = 7.4). They were stored in refrigerator for further characterization.

Synthesis of Nanocomposites: "Click" Chemistry. Nanocomposites were synthesized following "click" chemistry as described earlier. Briefly, the equivalent amount of alkynated metallic (cerium oxide and iron oxide) or HBPE nanoparticles (**11**) were mixed with equivalent amount of azide-functionalized HBPE nanoparticles (12) in the presence of catalytic amount of CuI and bicarbonate buffer (pH = 8.5), incubated at room temperature for 12 h. The resulting fluorescent HBPE nanocomposite and nanocomposite containing cerium oxide were purified using a PD-10 column, whereas magnetic nanocomposite containing iron oxide were purified using a magnetic column and finally dialyzed (MWCO 6−8K) against PBS solution (pH = 7.4). Nanocomposites were stored in a refrigerator for further characterization.

***In Vitro* Cell Studies.** *Cell Cultures*. Human lung cancer cells (A549) and rat cardiomyocytes (H9c2, noncancer) were obtained from ATCC, and maintained in accordance to the supplier's protocols. Briefly, the A549 cells were maintained in a 5%-FBS-containing DMEM medium supplemented with antimycotic/antibiotic, whereas the H9c2 cells were propagated in a 10%-FBS-containing MEM medium containing antimycotic/antibiotic. Cells were grown in a humidified incubator at 37 °C under 5% CO_2 atmosphere.

Confocal Laser-Scanning Microscopy. H9c2 and A549 cells were grown overnight on culture dishes, before treatment. After incubation with the nanoparticles, the cells were washed three times with 1X PBS, fixed with 5% formalin solution, and stained with DAPI (Molecular Probes). Subsequently, the cells were examined with a Zeiss LSM 510 confocal microscope equipped with a 40× objective.

MTT Assay. A549 and H9c2 cells (2,500 cells/well) were seeded in 96-well plates, incubated with HBPE nanoparticles for 6 h at 37 °C. Then, each well was washed three times with 1× PBS and treated with 20 μL of MTT (5 μg/μL) for 2 h. The resulting formazan crystals were dissolved in acidified isopropanol (0.1 N HCl) and the absorbance was recorded at 570 and 750 nm (background), using a Synergy HT multidetection microplate reader (Biotek). These experiments were performed in triplicates.

Flow Cytometry. A549 cells were grown until reaching confluence and then incubated with HBPE nanoparticles. After detachment and centrifugation at 1000 rpm, the cell pellets were

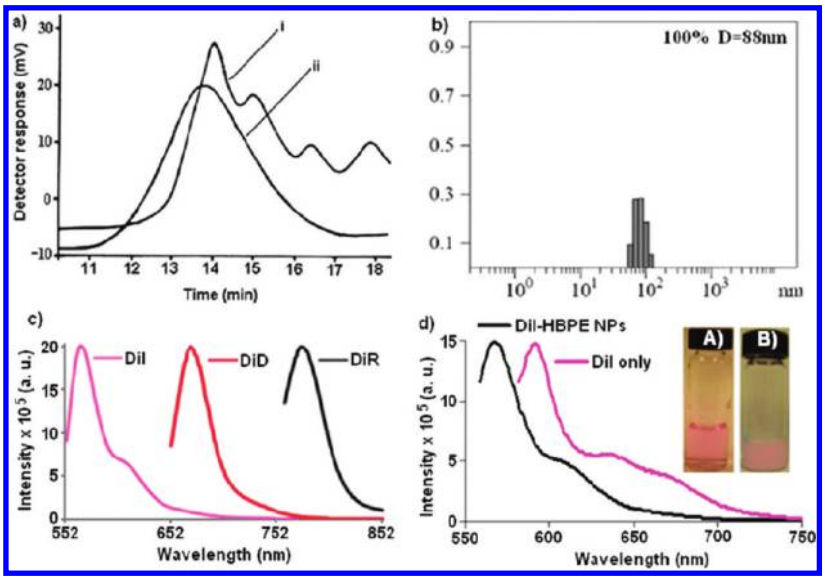

Figure 1. Characterization of HBPE **5** and HBPE nanoparticles **9**. (a) GPC traces of HBPE **5**, showing the formation of (i) oligomers and low-molecular weight polymers before applying vacuum and (ii) high molecular weight polymer after applying vacuum. (b) Determination of the hydrodynamic diameter of HBPE nanoparticles **9** using DLS, showing an average diameter of 88 nm. (c) Fluorescence emission spectra of different dye (DiI, DiD, and DiR)-encapsulated HBPE nanoparticles (**9**) in PBS buffer. (d) Comparing the fluorescence emission spectrum of DiI-HBPE NPs (**9**) with that of free DiI dye in solution. Inset: images showing (A) DiI dye alone in DMF solution and (B) DiI encapsulating HBPE nanoparticles (**9**) in PBS.

collected and resuspended in 1× PBS and the cellular suspensions were examined using a FACSCalibur flow cytometer (BD Biosciences).

IVIS Analysis. A total of 10 000 lung carcinoma cells were incubated for 6 h with the corresponding HBPE nanoparticles, and the supernatant was collected in Eppendorf tubes. Cells were thoroughly washed with 1X PBS, and detached as stated above. The resulting pellets were resuspended in 1 mL culture media. All Eppendorf tubes were examined simultaneously on a Xenogen IVIS system, using the ICG filter for DiR dye. All experiments were performed in triplicates.

In Vitro Drug/Dye Release. The *in vitro* drug/dye release studies were carried out using a dynamic dialysis technique at 37 °C. Briefly, 100 μL of HBPE nanoparticles (**13**) were incubated with porcine liver esterase (20 μL) inside a dialysis bag (MWCO 6−8 K), which was then placed in a PBS solution (pH 7.4). The amount of guest (dye or drug) molecules released from the nanoparticle into the PBS solution was determined at regular time intervals by taking 1 mL aliquots from the PBS solution and measuring the fluorescence intensity at 582 nm for DiI and 378 nm for Taxol. The concentration of the either dye or drug was calculated using a standard calibration curve. The cumulative fraction of release versus time was calculated using the following equation:

$$\text{cumulative release } (\%) = [\text{guest}]_t/[\text{guest}]_{\text{total}} \times 100$$

where $[\text{guest}]_t$ is the amount of guest released at time t, and $[\text{guest}]_{\text{total}}$ is the total guest present in the guest encapsulated HBPE nanoparticles.

Results and Discussion

Synthesis of the HBPE polymer (**5**) was achieved by the selective mono-C-alkylation of a readily available diethyl malonate **1** with bromobutyl acetate **2** to yield the monosubstituted compound **3** (Scheme 2). This monosubstitution reaction was controlled by using a weak base, such as potassium carbonate, and equivalent amount of starting materials. It should be noted that when the weak base was substituted with a strong base, like KOH or NaOH, the corresponding disubstituted product was obtained, which is unsuitable for further polymerization as it will eventually form undesired cross-linked byproducts. Next, the monosubstituted product **3** was subjected to basic hydrolysis using NaOH as a base and a mixed solvent (methanol/water) approach. Note that use of water should be avoided in the work-up stage as the hydrolyzed product **4** was highly soluble in water. The resulting novel AB_2 monomer (**4**) has three-bond connectivity with two carboxylic acid groups and one hydroxyl group in the structure (Scheme 1), which upon melt-polymerization produced a three-dimensional water-insoluble HBPE polymer **5** (see Experimental Section and the Supporting Information, section S1, for detailed synthesis protocols and characterizations). The as-synthesized HBPE polymer is highly branched and the presence of ester linkages in the three-dimensional polymeric backbone makes this polymer biodegradable.[10,16,17] The amphiphilic nature of the HBPE polymer **5** derives from the presence of hydrophobic moieties in the inner polymeric backbone, whereas polar groups are found at the surface. Upon dispersion in an aqueous environment, this HBPE polymer self-assembles, bringing the hydrophobic areas together to minimize contact with the aqueous environment, while exposing the hydrophilic segments containing the polar carboxylic acid groups to the aqueous media. These properties make our HBPE polymer important and attractive, particularly for biomedical applications, as this branched polymer is suitable for the fabrication of functional polymeric nanoparticles via the water-based solvent diffusion method (Schemes 1 and 2). This is contrary to microemulsion techniques utilized for the synthesis of nanoparticles made of commercially available polymers. In addition, our synthesized biodegradable branched polymer can be easily fine-tuned for the construction of multifunctional HBPE nanoparticles with diverse surface functionalization and encapsulating payloads. Our HBPE polymer, contrary to the conventional linear polymers, is amorphous, highly

(16) Kaihara, S.; Matsumura, S.; Mikos, A. G.; Fisher, J. P. *Nat. Protoc.* **2007**, *2*, 2767–2771.

(17) (a) Wang, C.; Ge, Q.; Ting, D.; Nguyen, D.; Shen, H. R.; Chen, J.; Eisen, H. N.; Heller, J.; Langer, R.; Putnam, D. *Nat. Mater.* **2004**, *3*, 190–196. (b) Li, S.-D.; He, J.-D.; Yu, P. H.; Cheung, M. K. *J. Appl. Polym. Sci.* **2003**, *89*, 1530–1536.

Table 1. Determination of Hydrodynamic Diameter (D) of Functional HBPE Nanoparticles (NPs) 13, Immediately after Synthesis[a]

NPs	D (nm)	DiI/NPs	DiD/NPs	DiR/NPs	Taxol/NPs	AzT/NPs	I_2−mol/NPs	Gd−DOTA/NPs
NP−DiI	88 ± 2	67 ± 4						
NP−DiD	89 ± 4		59 ± 4					
NP−DiR	91 ± 1			53 ± 2				
NP−Tax + DiI	92 ± 1	47 ± 2			24 ± 3			
NP−AzT + DiI	90 ± 3	44 ± 3				29 ± 4		
NP−I_2−mol	91 ± 3						58 ± 3	
NP−Gd−DOTA	89 ± 1							69 ± 6

[a] Quantitative estimation of amount of dyes (DiI, DiD, and DiR), Taxol, AzT, iodinated molecule and Gd−DOTA per HBPE nanoparticles (NPs) were performed using UV/vis spectroscopy. Folate per HBPE nanoparticle was 74 ± 5 in folate decorated NPs (D = 93 ± 2 nm).

branched, soluble, and biocompatible and has numerous surface functional groups for targeting and hydrophobic cavities for effective encapsulation of guest molecules, suggesting its versatility in biomedical applications.

Our first generation HBPE polymer **5** can be used as is, in order to make HBPE nanoparticles with carboxylic groups on their surface (**9**). Also **5** can be further post-functionalized (**6**−**8**) to yield surface aminated (**10**), alkynated (**11**) or azide-functionalized (**12**) HBPE nanoparticles (Scheme 2) using carbodiimide chemistry. The molecular weight of HBPE **5** was determined using Gel Permeation Chromatography (GPC) and showed the formation of high molecular weight polymer (M_w = 42 000, PD = 1.6) after applying vacuum (Figure 1a). All monomers and polymers were further characterized by ^{1}H and ^{13}C NMR, Mass and FTIR spectroscopies (Supporting Information Figures S1 and S2). Thermal gravimetric analysis (TGA) showed moderate thermal stability (10% weight loss at 250 °C in air) of the polymer, an excellent property for a biodegradable polymer[17] (Supporting Information Figure S3). The resulting HBPE polymers (**5**−**8**) were utilized to synthesize a series of functionalized HBPE nanoparticles (**9**−**12**) containing various types of cargos.

In our first set of experiments, we have encapsulated a series of hydrophobic fluorescent dyes (DiI, DiD and DiR, 10 μg/μL), drugs (Taxol and AzT, 1 μg/μL), chelated metals (Gd−DOTA, 25 μg/μL) and iodinated molecules (50 μg/μL) in the HBPE nanoparticles (**9**−**12**, Scheme 2). In brief, the polymer (20 mg) and cargo (5 μL) were dissolved in DMF (500 μL), a polar solvent, and added dropwise to the stirring DI water (5 mL), driving both the self-assembly and encapsulation processes and resulting in the formation of functional HBPE nanoparticles. Upon dispersion in an aqueous environment, the synthesized HBPE polymer self-assemble bringing the hydrophobic areas and hydrophobic cargos together to minimize contact with the aqueous environment, while exposing the hydrophilic segments containing carboxylic groups to the aqueous solution. These properties make our HBPE polymers suitable for the fabrication of HBPE nanoparticles via the solvent diffusion method. In this method, both the polymer and hydrophobic cargos to be encapsulated are dissolved in water-miscible organic solvents (DMF or DMSO) and the solution is added dropwise to an Eppendorf tube containing water under constant stirring. Under these conditions, the miscible solvent rapidly diffuses into the water, causing the polymer to self-assemble by bringing the hydrophobic areas together, therefore creating hydrophobic nanocavities that encapsulate the hydrophobic molecule, while exposing hydrophilic segments to the aqueous solution. This procedure results in the formation of carboxyl-functionalized spherical polymeric nanoparticles suspended in an aqueous environment that can be easily functionalized using facile carbodiimide chemistry. Scanning electron microscopy of the HBPE nanoparticles confirms the spherical geometry of the nanoparticles (Supporting Information, Scheme S1).

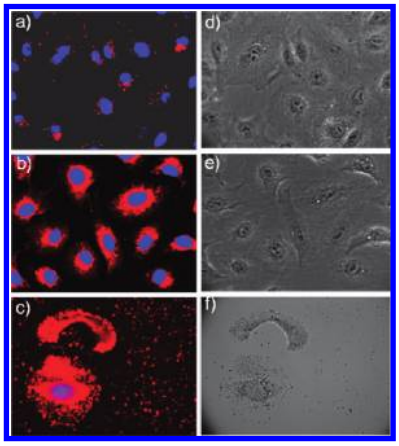

Figure 2. Assessment of DiI-encapsulating HBPE nanoparticles' cellular uptake via confocal laser-scanning microscopy. (a) No internalization was observed in cells incubated with carboxylated HBPE nanoparticles (**9**); (b) enhanced internalization was observed with folate-clicked HBPE nanoparticles (**13**). Cells incubated with (c) Taxol-encapsulating folate HBPE nanoparticles (**13**) induced Taxol-mediated mitotic arrest, leading to cell death, with the (d−f) corresponding bright field confocal images of the A549 cells treated with the corresponding functional HBPE nanoparticles. Nuclei stained with DAPI (blue). These observations confirmed the targeting capability and receptor-mediated internalization of our theranostic HBPE nanoparticles.

All HBPE nanoparticles were purified using a PD-10 column and dialysis (MWCO 6−8K) against PBS solution (pH = 7.4). These HBPE nanoparticles were highly stable in aqueous buffered solutions for more than a year, without significant precipitation or reduction in the fluorescence emission when concentrated (Supporting Information, Figure S4). Dynamic light scattering experiment confirmed the presence of stable and monodispersed HBPE nanoparticles with hydrodynamic diameter of 88 ± 2 nm (Figure 1b). The presence of different surface functional groups and encapsulation of cargos in the HBPE nanoparticles hydrophobic cavities was confirmed by FTIR, ζ-potential, spectroscopic analysis (Supporting Information, Figures S5−S8), and fluorescence experiments where the presence of fluorescence emission maxima at 570, 675, and 780 nm confirmed the encapsulation of DiI, DiD and DiR dyes inside the cavities (Figure 1c). Encapsulation of cargos inside the HBPE nanoparticles cavity was further confirmed by observing a shift[18,19] of 23 nm (Figure 1d) in the HBPE nanoparticle encapsulating DiI as compared to the free dye in solution. Amount of dyes, drugs, iodinated molecule, and Gd−DOTA per HBPE nanoparticle

(18) Shi, M.; Wosnick, J. H.; Ho, K.; Keating, A.; Shoichet, M. S. *Angew. Chem., Int. Ed. Engl.* **2007**, *46*, 6126–6131.
(19) Imaz, I.; Hernando, J.; Ruiz-Molina, D.; Maspoch, D. *Angew. Chem., Int. Ed.* **2009**, *48*, 2325–2329.

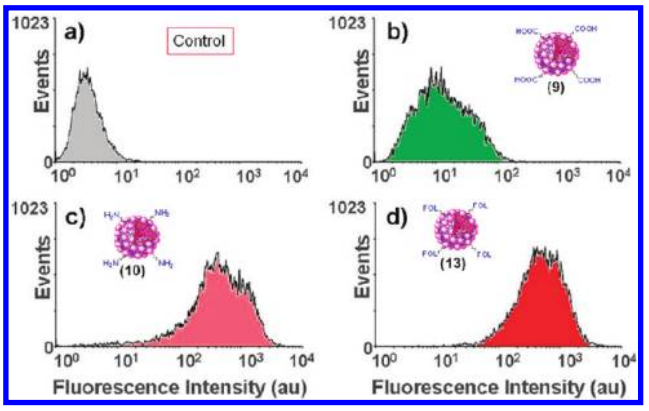

Figure 3. Assessment of HBPE nanoparticles' cell association via flow cytometry (FACS). (a) Absence of fluorescence emission was observed in control untreated A549 cells (1X PBS), whereas (b) partial association was observed for carboxylated HBPE nanoparticles (**9**). (c) Aminated (**10**) and (d) folate-clicked (**13**) nanoparticles interacted more profoundly with the cells, as indicated by higher levels of fluorescence emission.

and hydrodynamic diameters were calculated, as previously described[20,21] (Table 1).

The resulting small library of functional polymeric nanoparticles with diverse surface functionalities, as well as different cargos, can be readily used or further functionalized with targeting ligands for the design of targeted therapeutics, imaging and sensing applications.[22] Furthermore, they can be used in the formation of supramolecular assemblies (nanocomposites) to design novel materials with multifunctional properties for applications in tissue engineering, sensing devices, photonics and catalysis.[4,23]

First, we examined the surface-charged-dependent cell internalization and cytotoxicity of our nanoparticles. The HBPE nanoparticles **9**−**12** (3.5 mg/mL) containing fluorescent DiI molecules as cargos were incubated with A549 lung carcinoma or H9c2 human cardiomyocyte cells (10,000 cells) for 6 h and confocal microscopy studies were performed. Results showed no internalization of the carboxylated (**9**, Figure 2a), alkynated (**11**) or azide-derivatized (**12**) HBPE nanoparticles and no associated toxicity, which was evaluated through the MTT assay (Supporting Information, Figures S9 and S10). In contrast, cellular internalization of the aminated HBPE (**10**) nanoparticles was observed, indicated by the presence of strong fluorescence in the cytoplasm of both A549 and H9c2 cells (Supporting Information, Figure S11).

However, when we conjugated the carboxylated (**9**) or alkynated (**11**) nanoparticles with folic acid via "click" chemistry[24−28] (Supporting Information, Scheme S2, Figure S12) and incubated the resulting folate HBPE nanoparticles (**13**) with A549 cells,

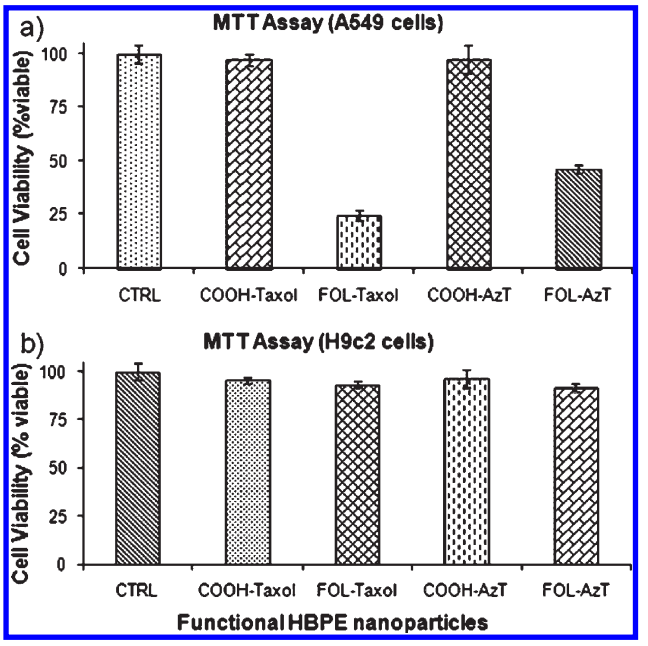

Figure 4. Determination of the theranostic HBPE nanoparticles' toxicity through the MTT assay. (a) The folate-decorated Taxol- and AzT-encapsulating HBPE nanoparticles induced a significant reduction in cell (A549) viability. (b) Determination of the specificity of the theranostic HBPE nanoparticles' toxicity using H9c2 cells. Results indicated no toxicity of the HBPE nanoparticles in H9c2 cells, does not overexpress folate receptor. Control cells were treated with 1× PBS. Average values of four measurements are depicted ± standard error.

which overexpress the folate receptor,[29,30] significant fluorescence in the cytoplasm was observed (Figure 2b). This contrasts with the results obtained with the corresponding parent nanoparticles (**9** and **11**) (Figure 2a, Supporting Information, Figure S10), which do not internalize in A549 cells. Flow cytometric (FACS) analysis corroborated these results, showing limited cell-associated fluorescence emission from cells treated with carboxylated HBPE **9** (Figure 3b), whereas a 3-fold increase in cell-associated fluorescence emission was observed in cells treated with the aminated HBPE nanoparticles **10** (Figure 3c) and folate HBPE nanoparticles **13** (Figure 3d) when compared to the control nontreated cells (Figure 3a). In addition, similar results were obtained in experiments using non-fixed A549 cells, where internalization of carboxylated (**9**) and folate-conjugated (**13**) HBPE nanoparticles were monitored using epifluorescence microscopy (Supporting Information, Figure S14). Experiments using live cells are important, as these studies confirmed that the observed enhanced fluorescence was due to the folate-conjugated fluorescence nanoparticles' internalizations in live cells and not a potential artifact due to cell-fixing. Meanwhile, internalization of **13** was nominal in A549 cells preincubated with free folic acid (Supporting Information, Figure S15), as well as in studies using H9c2 cardiomyocytes, a cell line that does not express the folate receptor[31] (Supporting Information, Figure S13b). These experiments confirmed the folate-receptor-mediated internalization of the folate-conjugated HBPE nanoparticles (**13**), whereas the aminated HBPE nanoparticles (**10**) showed nonspecific cellular internalization.

(20) Koch, A. M.; Reynolds, F.; Kircher, M. F.; Merkle, H. P.; Weissleder, R.; Josephson, L. *Bioconjug. Chem.* **2003**, *14*, 1115–1121.
(21) Shen, T.; Weissleder, R.; Papisov, M.; Bogdanov, A., Jr.; Brady, T. J. *Magn. Reson. Med.* **1993**, *29*, 599–604.
(22) Kim, I. B.; Bunz, U. H. *J. Am. Chem. Soc.* **2006**, *128*, 2818–2819.
(23) Kim, I. B.; Dunkhorst, A.; Gilbert, J.; Bunz, U. H. F. *Macromolecules* **2005**, *38*, 4560–4562.
(24) Sun, E. Y.; Josephson, L.; Weissleder, R. *Mol. Imaging*. **2006**, *5*, 122–128.
(25) Bachovchin, D. A.; Brown, S. J.; Rosen, H.; Cravatt, B. F. *Nat. Biotechnol.* **2009**, *27*, 387–394.
(26) Kolb, H. C.; Finn, M. G.; Sharpless, K. B. *Angew. Chem., Int. Ed. Engl.* **2001**, *40*, 2004–2021.
(27) Santra, S.; Kaittanis, C.; Grimm, J.; Perez, J. M. *Small* **2009**, *5*, 1862–1868.
(28) Englert, B. C.; Bakbak, S.; Bunz, U. H. F. *Macromolecules* **2005**, *38*, 5868–5877.
(29) Yuan, H.; Miao, J.; Du, Y. Z.; You, J.; Hu, F. Q.; Zeng, S. *Int. J. Pharm.* **2008**, *348*, 137–145.
(30) Nelson, M. E.; Loktionova, N. A.; Pegg, A. E.; Moschel, R. C. *J. Med. Chem.* **2004**, *47*, 3887–3891.
(31) Parker, N.; Turk, M. J.; Westrick, E.; Lewis, J. D.; Low, P. S.; Leamon, C. P. *Anal. Biochem.* **2005**, *338*, 284–293.

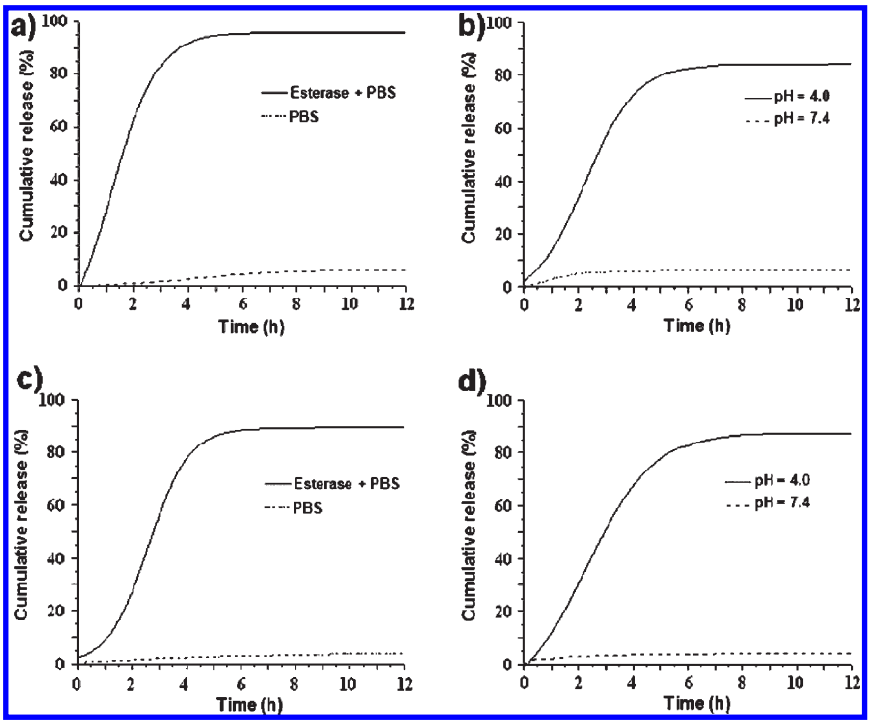

Figure 5. Drug and dye release profiles of Taxol and DiI coencapsulating HBPE nanoparticles (**13**) in PBS (pH = 7.4) at 37 °C. Release of Taxol (a and b) and DiI (c and d) were observed in the presence of an esterase enzyme (a and c) and at pH 4.0 (b and d).

Internalization of either aminated (**10**) or folate (**13**) HBPE nanoparticles in A549 lung carcinoma exhibited nominal cytotoxicity (Supporting Information, Figure S9), demonstrating their biocompatibility and non-toxicity even when internalized by the cells. However, when folate-conjugated HBPE nanoparticles (**13**) were loaded with Taxol, a cell microtubule synthesis inhibitor commonly used in cancer chemotherapy,[32−34] 75% cell death was observed in A549 cells (MTT assay, Figure 4a). Meanwhile, when AzT, a viral reverse transcriptase[35] and human telomerase[36] inhibitor, was encapsulated into the nanoparticles (**13**), 55% cell death was observed (A549 cells, Figure 4a). Overall, these data suggested that the induction of cell death was mainly mediated by either Taxol or AzT and not by the fluorophores. In contrast, no significant cytotoxicity was observed when H9c2 cells, were treated with the Taxol- or AzT-encapsulating nanoparticles (**13**), confirming their exclusive folate-receptor-mediated internalization (Figure 4b). Furthermore, these results suggest that the coencapsulation of a fluorophore and a therapeutic agent in our HBPE nanoparticles can be utilized for cellular targeting, such as in cancer or anti-HIV $CD4^+$-specific therapeutic regimes and visualization of tumor regression in clinical studies. The internalization and cytotoxicity effects of either the Taxol or AzT HBPE nanoparticles (**13**) were confirmed using confocal microscopy, showing the induction of significant mitotic arrest, leading to dramatic morphological changes and cell death (Taxol, Figure 2c). This observation indicated that Taxol's therapeutic efficacy was preserved, despite its HBPE nanoparticle encapsulation and strongly supports the importance of encapsulating this potent antitumor agent within the polymeric cavity and targeting its delivery, in order to prevent damage of nontransformed cells and healthy tissue. In another set of experiments, as most lung carcinomas exhibit aberrant telomerase activity, we found that the reverse transcriptase inhibitor AzT, encapsulated in HBPE nanoparticles (**13**), induced significant cell death, presumably via inhibition of telomerase activity (Supporting Information, Figure S16). Taken together, these findings support the principle that folate-decorated HBPE nanoparticles can target and deliver chemotherapeutic agents to folate-receptor-overexpressing carcinomas, while visualizing the drug's homing.

The therapeutic applications of our HBPE nanoparticles rely on the biodegradability and biocompatibility of the nanoparticles, and most importantly, on the rate of release of the encapsulated drug from the polymeric nanocavities. To evaluate the HBPE nanoparticles' (**13**) drug release profile, we performed enzymatic (esterase from porcine liver) and low-pH degradation experiments using a dynamic dialysis technique at 37 °C. Results indicated that Taxol (Figure 5a,b) was released faster than the dye (Figure 5c,d) when the nanoparticles were incubated with either an esterase or at low pH 4.0. These differential release profiles may be attributed to the drug's size and its hydrophobic nature. As nominal cargo release was observed at physiological pH, we deduced that the HBPE nanoparticles should be stable under these conditions, whereas they are readily biodegraded upon enzymatic and intracellular environmental triggers, such as localization in acidified lysosomal compartments. Taken together, these results indicate the efficient drug release capability of our theranostic HBPE nanoparticles, rendering targeted HBPE nanoparticles useful for potential *in vivo* applications.

For *in vivo* imaging applications, nanoparticles with excitation and emission in the near-infrared region (650−900 nm) are needed for deep tissue fluorescence imaging.[37] Toward this end, DiR (excitation/emission: 751/780 nm) encapsulating carboxylated (**9**) and folate (**13**) HBPE nanoparticles were incubated with

(32) Davis, M. E.; Chen, Z. G.; Shin, D. M. *Nat. Rev. Drug. Discov.* **2008**, *7*, 771–782.
(33) Fonseca, C.; Simoes, S.; Gaspar, R. *J. Controlled Release* **2002**, *83*, 273–286.
(34) Gupte, A.; Ciftci, K. *Int. J. Pharm.* **2004**, *276*, 93–106.
(35) Shen, L.; Peterson, S.; Sedaghat, A. R.; McMahon, M. A.; Callender, M.; Zhang, H.; Zhou, Y.; Pitt, E.; Anderson, K. S.; Acosta, E. P.; Siliciano, R. F. *Nat. Med.* **2008**, *14*, 762–766.
(36) Datta, A.; Nicot, C. *Oncogene* **2008**, *27*, 1135–1141.
(37) Weissleder, R.; Ntziachristos, V. *Nat. Med.* **2003**, *9*, 123–128.

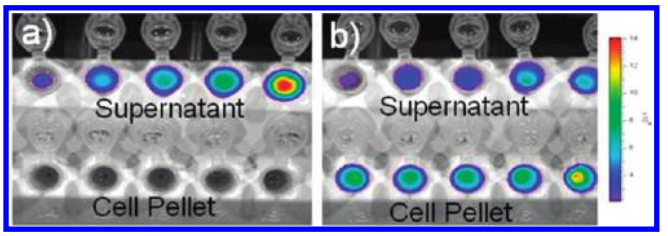

Figure 6. Fluorescence images of the cellular uptake of DiR-encapsulating (a) carboxylated (**9**) and (b) folate-derivatized (**13**) HBPE nanoparticles taken from a Xenogen IVIS system.

A549 cells for 6 h and imaged with an *in vivo* imaging system (IVIS), using an ICG filter set (Figure 6). No cell-associated fluorescence was observed in cells treated with carboxylated HBPE nanoparticles **9** (Figure 6a), whereas a dose-dependent increase in fluorescence was observed in cells treated with the folate HBPE nanoparticles **13** (Figure 6b), demonstrating receptor-mediated internalization and *in vivo* imaging capability. Taken together, these findings support the principle that our HBPE nanoparticles can be used in imaging and therapeutic applications in targeted delivery of chemotherapeutic agents, visualization of drug's homing and monitoring of drug release.

The unique properties of the HBPE nanoparticles, such as (a) encapsulation of diverse cargos, (b) different surface functionalization, and (c) stability at physiological pH with selective biodegradability and cargo release upon enzymatic or low pH triggers, make them ideal nanomeric units for the creation of supramolecular assemblies and nanocomposites. In recent years there has been an interest in the synthesis of polymeric nanocomposites with unique magnetic, luminescent and radiation-protection properties that are different from the bulk properties of the same material. Particularly, the creation of multifunctional implantable materials for application in tissue engineering or implantable devices with signal-driven cargo release is an emerging field. Therefore, we hypothesized whether our HBPE nanoparticles, particularly the ones conjugated with azide or alkyne surface moieties (clickable polymeric nanoparticles) would self-assemble among themselves or with other metallic nanoparticles (using "click" chemistry) to create novel polymeric or polymeric-metallic nanocomposites with enhanced magnetic or radiopacity properties for MRI and X-ray-CT applications, enhanced fluorescence, catalytic activities, radical scavenging and anti-inflammatory properties for tissue engineering.

Toward this goal, we first facilitated the self-assembly of two sets of HBPE nanoparticles, one encapsulating a hydrophobic iodinated molecule (5-amino-2,4,6-triiodoisophthalic acid, Supporting Information, Figure S17) with alkyne-functionalized surface (**11**) and a second one encapsulating a fluorescent dye (DiR, Supporting Information, Figure S18) with azide-functionalized surface (**12**). We have chosen the triiodinated compound, because it is an important synthon for the synthesis of radiopaque molecules for X-ray CT imaging,[38] is used for radio labeling of proteins[39] and can be easily encapsulated inside the polymeric nanocavities due to the presence of an extensive hydrogen-bonding network. The resulting two sets of clickable nanoparticles self-assemble upon addition of CuI as catalyst, forming a HBPE nanocomposite with both radiopaque (Figure 7a) and fluorescent (Figure 7b) properties. Absence of X-ray contrast was observed in control nanoparticle assemblies composed of HBPE nanoparticles without iodinated molecule (Figure 7a: X-i and Z-i)

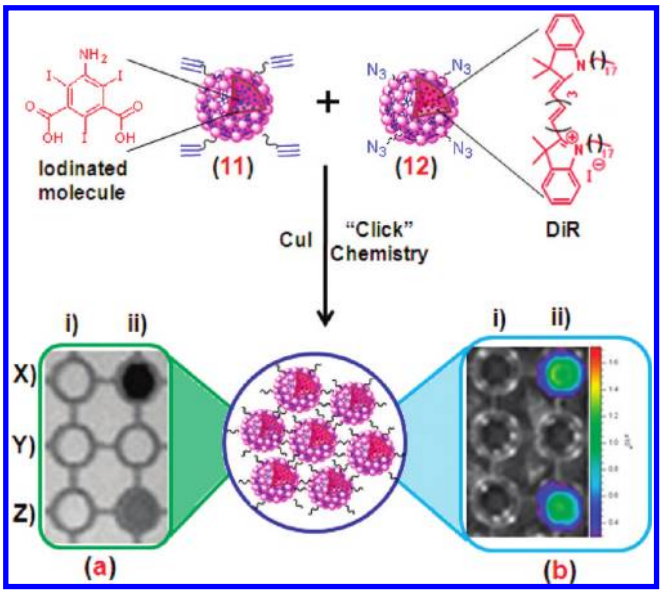

Figure 7. Schematic representation of the "click" chemistry mediated water-based syntheses of an X-ray blocking (a) and highly fluorescent (b) polymeric nanocomposite (NCs) encapsulating a tri-iodinated molecule and DiR, respectively. Nanocomposites without iodinated molecule (a: X-i and Z-i) and DiR (b: X-i and Z-i) showed no X-ray blocking and fluorescence properties, respectively. Y−I and Y-ii contained PBS.

Figure 8. Schematic representation of the syntheses of a magnetic and fluorescent (a) and free radical scavenging (b) polymeric-metallic nanocomposite (NCs) containing iron oxide and cerium oxide nanoparticles, respectively, using "click" chemistry.

or in phosphate buffered solution (Figure 7a: Y-i, ii). Similarly, no fluorescence was observed in nanoassemblies without DiR dye (Figure 7b: X-i and Z-i) and in phosphate buffered solution (Figure 7b: Y-i, ii). In addition, nanocomposites containing a fluorescent dye and a chelated metal (Gd−DOTA) were developed, demonstrating the capability of our system to create HBPE nanocomposites containing chelated metals for applications in imaging and catalysis.

Similarly, a nanocomposite can be engineered with a mixture of HBPE and metallic nanoparticles. For these studies clickable iron oxide[27] and cerium oxide[40] nanoparticle derivatized with alkyne groups were prepared, as previously reported, and conjugated with azide-functionalized HBPE nanoparticle encapsulating DiR (**12**).

(38) Beck, T.; Sheldrick, G. M. *Acta Crystallogr.* **2008**, *E64*, o1286.
(39) Ogan, M.; Tomasella, F. P.; Tu, J.-I. US patent 5463080, **1992**.
(40) Asati, A.; Santra, S.; Kaittanis, C.; Nath, S.; Perez, J. M. *Angew. Chem., Int. Ed. Engl.* **2009**, *48*, 2308–2312.

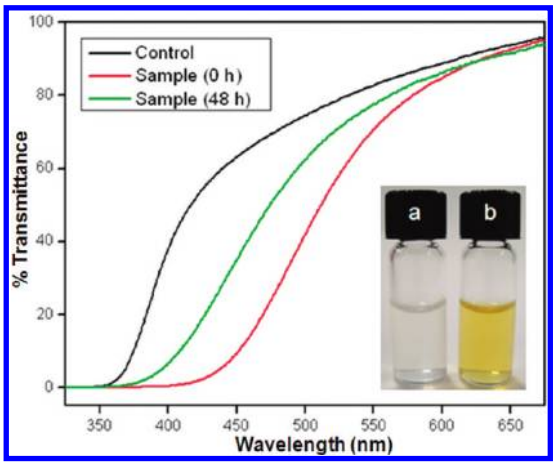

Figure 9. Autocatalytic activity of nanocomposite containing cerium oxide nanoparticles. Upon addition of hydrogen peroxide, a rapid color change from clear (a) to yellow (b) was observed, corresponding to a concomitant red shift in the UV/vis transmittance spectrum. Gradually, as the system regenerated a shift in the transmittance curve toward its original control value was seen.

When alkynated iron oxide nanoparticles were assembled via "click" chemistry with the azide HBPE fluorescent nanoparticle, a nanocomposite with dual fluorescent and magnetic properties was obtained (Figure 8a). By incorporating magnetic nanoparticles into the HBPE composite, a fluorescent material that can be controlled by an external magnetic field is obtained. It is also worth noticing that the localization, and integrity of an implantable material made with this composite could be potentially visualized in deep tissue through magnetic resonance imaging (MRI) and optical imaging. Subsequently, when alkynated cerium oxide (ceria) nanoparticles were used to create the nanoassembly, a composite with enhanced fluorescent properties and resistant to UV-induced photobleaching was obtained (Figure 8b). Results using this nanocomposite showed enhanced photostability of the DiR's near-infrared fluorescence within the nanocomposite (DiR−Ce−NCs, Figure 8b) as compared to the photostability of the dye in the fluorescent nanoparticles (DiR−NPs) or DiR dye in solution. The dye's photobleaching in the absence of ceria may be attributed to the generation of reactive oxygen species (ROS) during UV irradiation. Therefore, in the cerium oxide-containing nanocomposite the photobleaching of the dye is prevented via a ceria-mediated mechanism, as cerium oxide nanoparticles have the ability to selectively scavenge ROS.[41−43]

In addition, this nanocomposite showed excellent autocatalytic and antioxidant activity (Figure 9) as expected due to the presence of cerium oxide nanoparticles. The ability of our cerium oxide containing nanocomposite to reversibly switch from Ce^{3+} to Ce^{4+} is a key factor for its catalytic and biological applications as antioxidants. We examined whether the formation of a nanoassembly compromised the ceria nanoparticles' autocatalytic behavior. In the UV/vis experiments, the transmittance spectra showed reversible autocatalytic behavior when incubated with H_2O_2 at pH 7.4 (black, control, before addition of H_2O_2; red, immediately after addition of H_2O_2; green, after 48 h). Upon addition of H_2O_2, a yellow color was observed rapidly, corresponding to the red shift in UV/vis transmittance spectrum (red curve), compared to the control (black curve). We observed a gradual shift of the transmittance curve to its original control value, demonstrating the reversibility and autocatalytic activity of the nanocomposite under normal physiological condition.

Summary

In summary, we have introduced a new class of hyperbranched polymer capable of forming a library of functional polymeric nanoparticles with dual diversity in the nanoparticle surface and cargo. The hyperbranched polymer was new in its class and used for the first time to synthesize theranostic nanoparticles and nanocomposites for biomedical applications. The presence of hydrophobic pockets inside the three-dimensional hyperbranched structures played an important role in the encapsulation of a variety of hydrophobic cargos such as fluorescent dyes, therapeutic agents, chelated metals and iodinated molecules using the solvent diffusion method. The resulting nanoparticles showed high solubility and stability of encapsulation of their respective cargos in aqueous buffered solutions, at physiological pH. Only an enzyme (esterase) or acidic pH triggered the release of the cargos at different rates (for example, drug vs dye). Furthermore, the resulting functional hyperbranched nanoparticles can be surface-modified with a variety of ligands for targeting and sensing applications. Also, the nanoparticles' surface functionality allows the formation of nanoparticle assemblies (nanocomposites) and multifunctional materials for the creation of smart responsive materials. These polymeric nanocomposites showed excellent magnetic, fluorescent, MRI imaging, X-ray contrast and catalytic activity when conjugated with dye encapsulating HBPE nanoparticles, iron oxide and cerium oxide nanoparticles. Our studies demonstrated the importance of our newly synthesized HBPE polymers, nanoparticles and nanocomposite as they are biodegradable, targetable, nontoxic, and have capability to encapsulate a wide range of guest molecules. This offers the possibility to create novel multifunctional materials composed of hyperbranched polymeric nanoparticles with unique properties that can be tailored by the nature of their cargo, their surface functionality, and the formation of supramolecular assemblies.

Acknowledgment. We thank Dr. Annette Khaled (UCF) and Mounir Chehtane (UCF) for assistance with FACS analysis, as well as Atul Asati (UCF) for assistance with the cerium oxide nanoparticle. This work was supported by NIH Grants CA101781 and GM084331 and UCF NSTC Start Up Fund, all to J.M.P.

Supporting Information Available: (1) synthesis and characterizations of monomers and polymers, (2) nanoparticle characterizations, (3) receptor-mediated cellular internalizations and determination of cytotoxicity using confocal microscopy and MTT assay, incuding figures showing NMR spectra, a TGA thermogram, structures and photos of the dyes, ζ-potential of **9** and **10**, FT-IR spectra, fluorescence emission spectra, determination of the HBPE nanoparticles' toxicity, microscopic images of cells, and UV/vis images, and schemes showing synthetic representations of the syntheses. This material is available free of charge via the Internet at http://pubs.acs.org.

(41) Chen, J.; Patil, S.; Seal, S.; McGinnis, J. F. *Nat. Nanotechnol.* **2006**, *1*, 142–150.
(42) Perez, J. M.; Asati, A.; Nath, S.; Kaittanis, C. *Small* **2008**, *4*, 552–556.
(43) Das, M.; Patil, S.; Bhargava, N.; Kang, J.-F.; Riedel, L. M.; Seal, S.; Hickman, J. J. *Biomaterials* **2007**, *28*, 1918–1925.